Volume 140, Issue 9, September 2018,
Article number 091204

CFD Investigation of a Core-Mounted-Target-Type Thrust Reverser, Part 1: Reverser Stowed Configuration

Tashfeen Mahmood[1]

Email: dr.tashfeenmahmood@gmail.com
Defence Equipment and Services, Ministry of Defence,
Bristol, BS34 8JH, UK

Anthony Jackson[2]

Email: a.j.b.jackson@cranfield.ac.uk
Cranfield University, Centre for Propulsion Engineering,
Bedfordshire, MK43 0AL, UK

Vishal Sethi[3]

Email: v.sethi@cranfield.ac.uk
Cranfield University, Centre for Propulsion Engineering,
Bedfordshire, MK43 0AL, UK

Bidur Khanal[4]

Email: b.khanal@cranfield.ac.uk
Cranfield University, Centre for Defence Engineering,
Shrivenham, SN6 8LA, UK

Fakhre Ali[5]

Email: fakhre.ali@chalmers.se
Chalmers University of Technology, Applied Mechanics Department,
Hörsalsvägen 7A, Göteborg, Sweden

[1] Engineering Manager
[2] Senior Research Companion
[3] Lecturer
[4] Lecturer
[5] Research Fellow

Abstract

During the second half of the 90's, NASA performed experimental investigations on six novel Thrust Reverser (TR) designs; Core Mounted Target Type Thrust Reverser (CMTTTR) design is one of them. To assess the CMTTTR efficiency and performance, NASA conducted several wind tunnel tests at Sea Level Static (SLS) conditions. The results from these experiments are used in this paper series to validate the CFD results.

This paper is part one of the three-part series; Part 1 and 2 discusses the CMTTTR in stowed and deployed configurations, all analysis in the first two papers are performed at SLS conditions. Part 3 discusses the CMTTTR in the forward flight condition.

The key objectives of this paper are: first, to perform the 3D CFD analysis of the reverser in stowed configuration; all analyses are performed at SLS condition. The second objective is to validate the acquired CFD results against the experimental data provided by NASA [1]. The third objective is to verify the fan and overall engine net thrust values acquired from the aforementioned CFD analyses against those derived based on 1-D engine performance simulations. The fourth and final objective is to examine and discuss the overall flow physics associated with the CMTTTR under stowed configuration.

To support the successful implementation of the overall investigation, full-scale 3D CAD models are created, representing a fully integrated GE-90 engine, B777 wing, and pylon configuration.

Overall a good agreement is found between the CFD and test results; the difference between the two was less than 5%.

Nomenclature

3D	=	Three Dimensional
BPR	=	Bypass Ratio
CAD	=	Computer Aided Design
CMTTTR	=	Core Mounted Target Type Thrust Reverser
CNE_{Area}	=	Core Nozzle Effective Area [m^2]
c_p	=	Constant pressure
CTTR	=	Cascade Type Thrust Reverser
CUTS_TF	=	Cranfield University Twin Spool Turbofan
DP	=	Design Point
FG_{Thrust}	=	Fan Gross Thrust [kN]
FNPR	=	Fan nozzle pressure ratio
FNE_{Area}	=	Fan Nozzle Effective Area [m^2]
GR_{Thrust}	=	Gross Reverse Thrust [kN]
HBPR	=	High Bypass Ratio
NASA	=	National Aeronautics and Space Administration
NR_{Thrust}	=	Net Reverse Thrust [kN]
PDTTR	=	Pivoting Door Type Thrust Reverser
Rev	=	Reverse
SLS	=	Sea Level Static
TTTR	=	Target Type Thrust Reverser
TET	=	Turbine Entry Temperature [K]
TO	=	Take-off
TR	=	Thrust Reverser
V_{bypass}/V_{Core}	=	Bypass to core flow velocity ratio
$\eta_{Propulsive}$	=	Propulsive Efficiency [%]
$\eta_{Thermal}$	=	Thermal Efficiency [%]

1. Introduction

THRUST REVERSERS (TRs) installed on civil subsonic aircraft engines are mainly deployed during the landing phase (i.e. at touchdown), typically for a short time period (i.e. 15 – 25 seconds) [2, 3]; TRs are also essential for emergency occasions such as aborted take-off. The main objective of any TR is to divert the engine exhaust flow such that it generates a decelerating force. TRs on medium to high bypass ratio (HBPR) turbofan engines are normally integrated onto the outer cowl of the engine nacelle (i.e. fan nacelle) and operate only on the bypass airstream. This is advantageous as approximately 80% of the forward thrust on a typical HBPR (e.g. BPR≈9) turbofan engine is generated from the bypass airstream [1].

TRs installed on HBPR engines weigh about 30% of the total nacelle weight: a typical example is the GE-90 engine which has a BPR≈9 and its TR weighs approximately 1500kg [1]. Despite their heavy weight and short operational times, TRs are universally incorporated on civil aircraft. TR design, certification, integration, and installation are challenging activities that both the aircraft and engine manufacturers have to undertake. TR deployment improves the overall safety of both the aircraft and passengers. Also, for all airports stopping the aircraft within the safe landing distances is essential, as there could be a risk to human life and to airport terminals and infrastructure. TR operation is also beneficial in airfields where the length of the runway is short. Furthermore, on wet or icy runways the performance of a TR is far superior to any other decelerating device (i.e. wheel brakes or lift dumpers).

A key performance requirement from any TR design is its ability to achieve at least ≈ 40% reverser effectiveness and in doing so it should have a minimum effect on the engine performance. For a pivoting door type thrust reverser (PDTTR) there are additional requirements such as maintaining the satisfactory runway clearance when deployed and designing an efficient control system which can ensure that if there is a mechanical failure, the reverser will return to the forward flight position.

Existing operational TR designs include the following:

1. Cascade Type Thrust Reverser (CTTR):

   CTTTR are generally incorporated on HBPR turbofan engines, (i.e. BPR ≥ 6) and are composed of the following parts: a translating cowl, hydraulic actuators, control system, reverser cascade blocks and a blocker door. During the deployment phase, the translating cowl will move aft and blocker doors

are deployed into the bypass section, such that they form the blockage; the bypass flow will then be diverted into the reverser cascade vanes. Subsequently, cascade vanes will then accelerate the flow in order to generate an effective reverse thrust, (Fig. 1).

2. Pivoting Door Type Thrust Reverser (PDTTR):

PDTTRs are generally incorporated on the medium BPR turbofan engines i.e. BPR≤6; typical engine examples are CFM56-6B and Trent 700. In terms of their operation, PDTTR exploits the inner surfaces of the blocker door along with a kicker plate to re-direct the flow in the forward direction (i.e. in the direction of oncoming air), (Fig. 1).

3. Target Type Thrust Reverser (TTTR):

TTTRs are generally incorporated on the low BPR mixed exhaust engines (i.e. BPR≈1). These types of TRs are designed such that when fully deployed they are at some distance aft of the exhaust nozzle with an aim to reverse the complete exhaust flow of the engine, (Fig. 1).

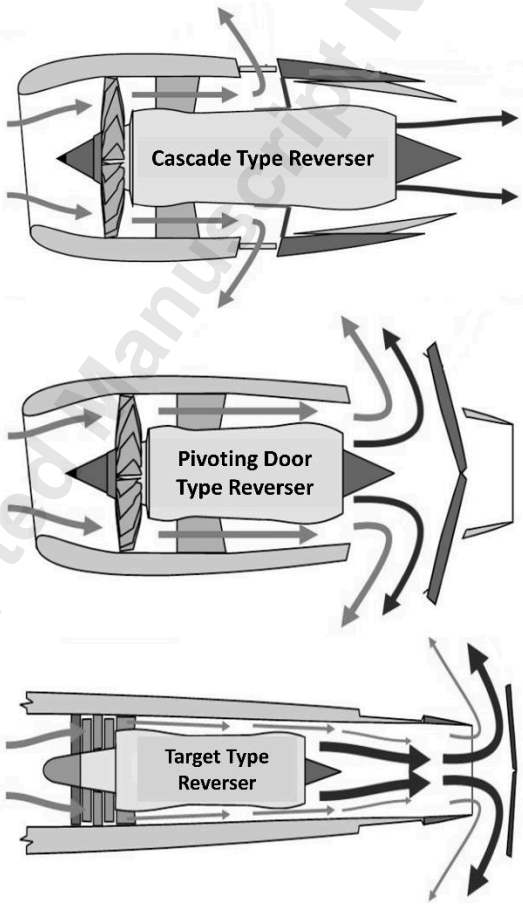

Fig 1: Existing thrust reverser designs on civil aircraft engines [12].

2. Employed Simulation Methodology

It is evident that the nature of the problem addressed within this research requires employment of multiple disciplines, demanding a combined effort in CAD and CFD. The overall methodology employed to support the research addressed herein is therefore accomplished by the following three broad steps:

(i) Compilation of the 3D CAD models corresponding to the engine, pylon, wing, runway, symmetry and far field boundaries as well as their integration and computational setup.

(ii) Mesh generation of the acquired 3D CAD models to support the execution of the CFD analyses.

(iii) The acquisition of the engine design and off-design performance parameters; values obtained from the engine performance study are used to setup the boundary conditions for the CFD cases.

2.1 Compilation of 3D CAD models and computational setup

The 3D CAD modeling is performed using CATIA V5 design software. The CAD models are first converted into an IGS format and later transferred to ICEM software for geometric cleaning and meshing. Due to the complexity of the CAD models (as there are several parts), it is important to ensure that the IGS models are free of surface errors i.e. all the points, curves and surfaces are fixed; this is an essential step before any meshing is performed.

NASA performed the wind tunnel experiments using a 7.9% scaled model of the GE90 engine; the engine model was integrated with the 7.9% scaled model of a B777 wing and pylon geometries [1]. A typical experimental setup used for the wind tunnel testing is shown in Fig. 2. During the experiments, air supplies for the core and bypass streams were handled using the primary and secondary lines. Air flow in each line was at a different pressure, as depicted in Fig. 3 [1]. The method of introducing supply lines is not practical for the implementation of CFD analyses. Therefore, for the CFD analyses, a complete full-scale 3D CAD model of the engine outer nacelle was built, incorporating the front section of the nacelle, together with fan inlet and outlet surfaces (thus replacing the supply lines).

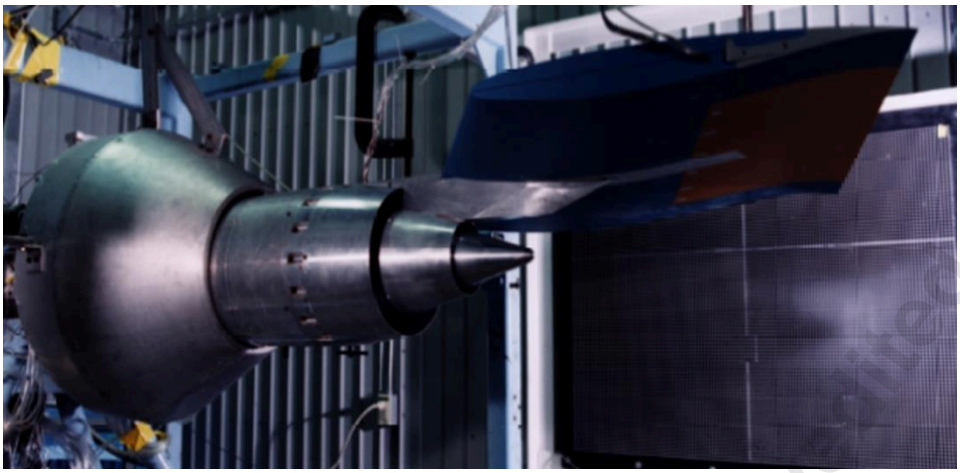

Fig. 2: Wind tunnel model of the TR in stowed configuration, adopted from [1].

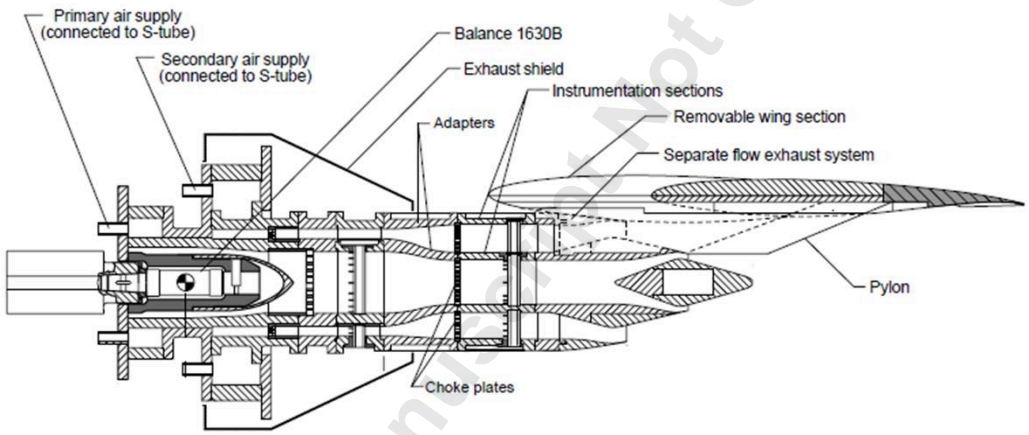

Fig. 3: Sketch of the Geometry schematic of NASA's experimental engine model [1].

In the experiments, the internal and external surfaces of the fan nacelle were symmetric. This assumption is strictly speaking not true for a real GE-90 engine as in reality, the fan nacelle external surface is flatter near the bottom; this is mainly due to the gearbox and TR installation and to avoid any flow re-ingestion during landing. Thus, for this CFD study, the fan nacelle outer surface is designed such that it represents a more realistic geometry. Other major engine components comprise of core inner and outer cowls, exhaust plug, nacelle frontal section, fan inlet and outlet surfaces, nose cone, and fan nacelle inner surface. The acquired full-scale 3D engine model, therefore, shares similar design characteristics to the NASA's 7.9% scale experimental model (apart from the fan outer nacelle). Figure 4 presents the engine CAD model when the reverser is stowed (i.e. forward thrust) condition.

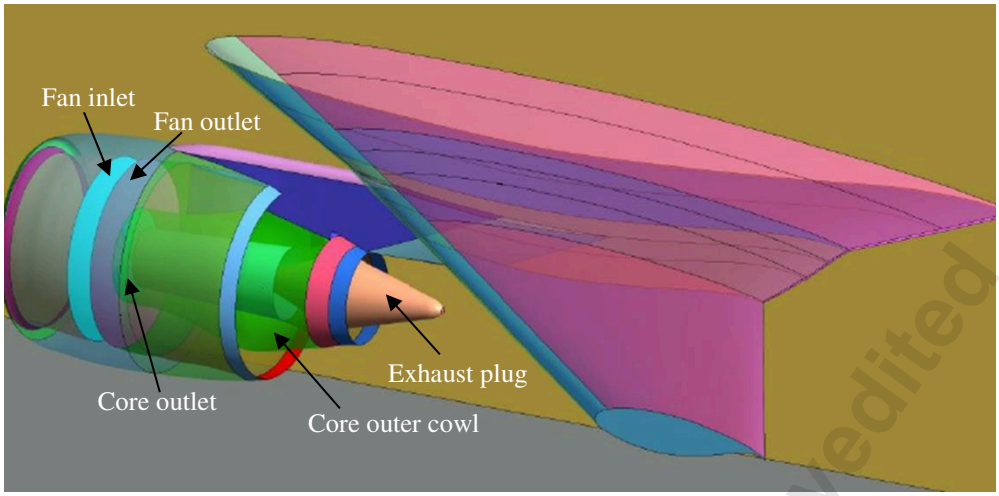

Fig. 4: Developed integrated 3D CAD model with TR in stowed configuration.

It is important for the CFD analyses that reasonably accurate dimensions are given to the following geometric features: fan inlet area, fan outlet area, fan nozzle exit area, core inlet area and core nozzle exit area. Since such information is not available in public domain, a commonly employed approach was adopted to derive an estimate of the aforementioned parameters from the engine 'design-point' performance study (tabulated in Table 1).

One of the key performance requirements for any TR design is to satisfy the mass flow compatibility criteria (i.e. if the fan pressure ratios and thrust settings remain unchanged, then the mass flow for both the reverser stowed and deployed configurations must be similar). This is an essential performance requirement, as it will ensure that the operating point on the compressor maps will not be far off in both the conditions. However, achieving this mass flow compatibility is difficult. This is mainly because the fan nozzle mass flow in the forward thrust configuration will mostly be axial, whereas, in the reverse thrust configuration the flow will first be forced to turn at an angle due to the presence of the blocker door and later will be guided using the TR surfaces. A common approach to fulfilling this mass flow compatibility criteria for the reverser deployed configurations is to iteratively find an 'effective reverser exit area' which will satisfy this condition. This 'effective reverser exit area', will be slightly larger than the forward thrust 'effective nozzle exit area'. This is an important consideration and must be investigated and is discussed in detail in Part 2 of this paper.

A runway is included for the CFD analyses (see Figs. 4 and 5); this will allow the flow physics associated with exhaust plumes and the ground to be captured. The value of runway clearance (i.e. the distance between the nacelle bottom surface and the runway) is set similar to that of the B777 employing a GE90 engine. The inclusion of a runway

offers an opportunity to thoroughly investigate not only the forward flight performance at landing but also the reverser flow physics under various thrust settings (discussed in Part 2); it will allow investigation of reverser problems, such as flow ingestion, temperature and pressure distortions and additional lift generation from the flow under the nacelle.

Another important requirement for successful execution of the CFD analyses is to have a sufficiently large flow domain. In a normal forward flight condition (i.e. when the reverser is stowed) fan and core exhaust jets will be axial and depend on the thrust settings: the engine exhaust flow can reach very high speed and can travel far downstream while retaining non-uniformity in the flow. It is therefore important that the downstream far-field boundary is set sufficiently far so that the exhaust flows weakens to free stream level. Similarly, during the reverse thrust operation, all the far-field boundaries must be set so that the domain size is sufficient to have a negligible effect on the overall flow. For these reasons the pressure far-fields in the upstream and downstream zones are set as ≈60 times the size of the wingspan, the height of the flow domain is ≈30 times the size of wing span (see Fig. 5). It should be noted that these dimensions are derived after conducting extensive 2D CFD analyses, based on which it was established that these dimensions are appropriate to sufficiently resolve the flow physics without any disturbances. A large rectangular box is built around the integrated CAD model (see Fig. 5). One side surface of this box will have a symmetric boundary condition, because the B777 is a twin-engine aircraft; all remaining surfaces are setup as pressure far-field. An isometric view of a complete 3D CAD model, employed for all CFD analyses executed under the scope of this research is presented in (Fig. 5).

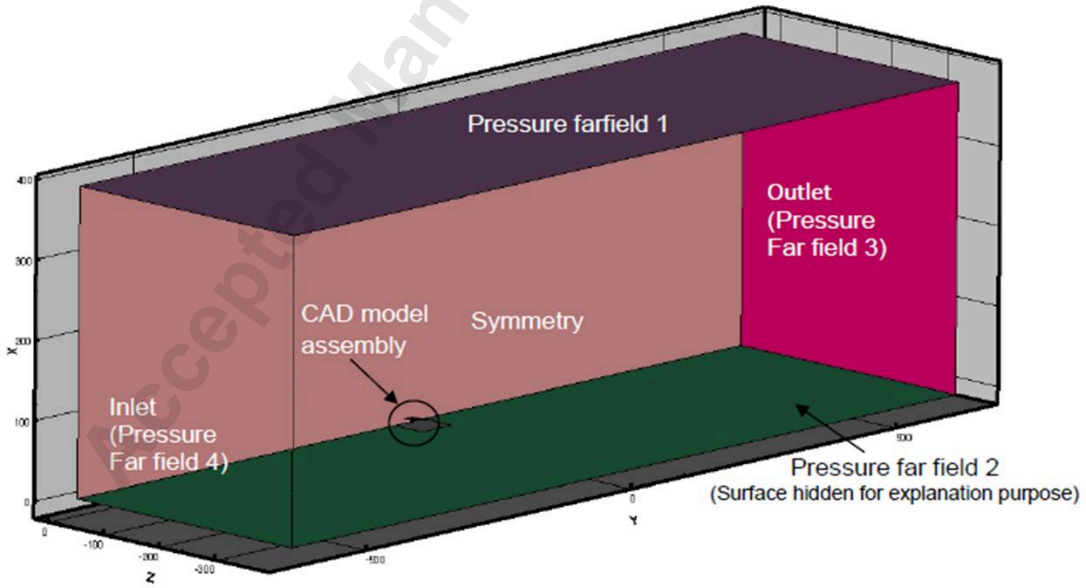

Fig. 5 An isometric view of the developed computational model employed for the CFD analyses.

2.2 Mesh Generation

Mesh is generated using the ANSYS ICEM software; unstructured meshing is used for all geometries. Initially, a surface mesh is created then the prism mesh is built, and finally the volume mesh is formed. Generation of the surface mesh was both laborious and time-consuming. In ICEM CFD surface mesh is generated either individually on each geometric part or simultaneously on all geometric parts. The latter approach is adopted, mainly because the translation from one geometric part to the next becomes considerably smooth. To capture the flow physics well, the number of mesh elements on geometric surfaces are well refined. Mesh sensitivity study established that ≈ 5.5 million mesh elements are sufficient to acquire a reasonable accuracy of results; this is in line with similar studies conducted in [5, 6 and 7]. Typical surface meshes are shown in Figs. 6a ,6b, 7a and 7b.

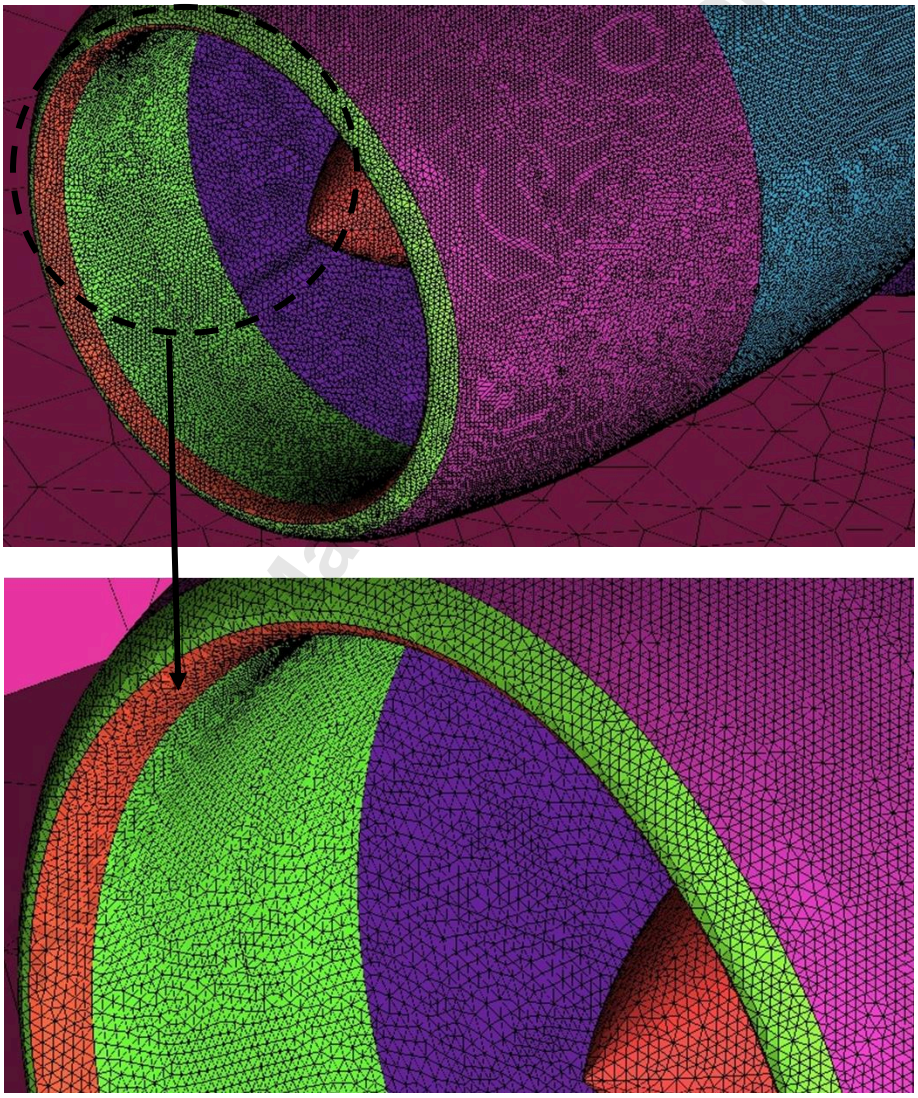

Fig. 6a: Surface mesh distribution around the nacelle. Fig 6b: Shows the magnified view.

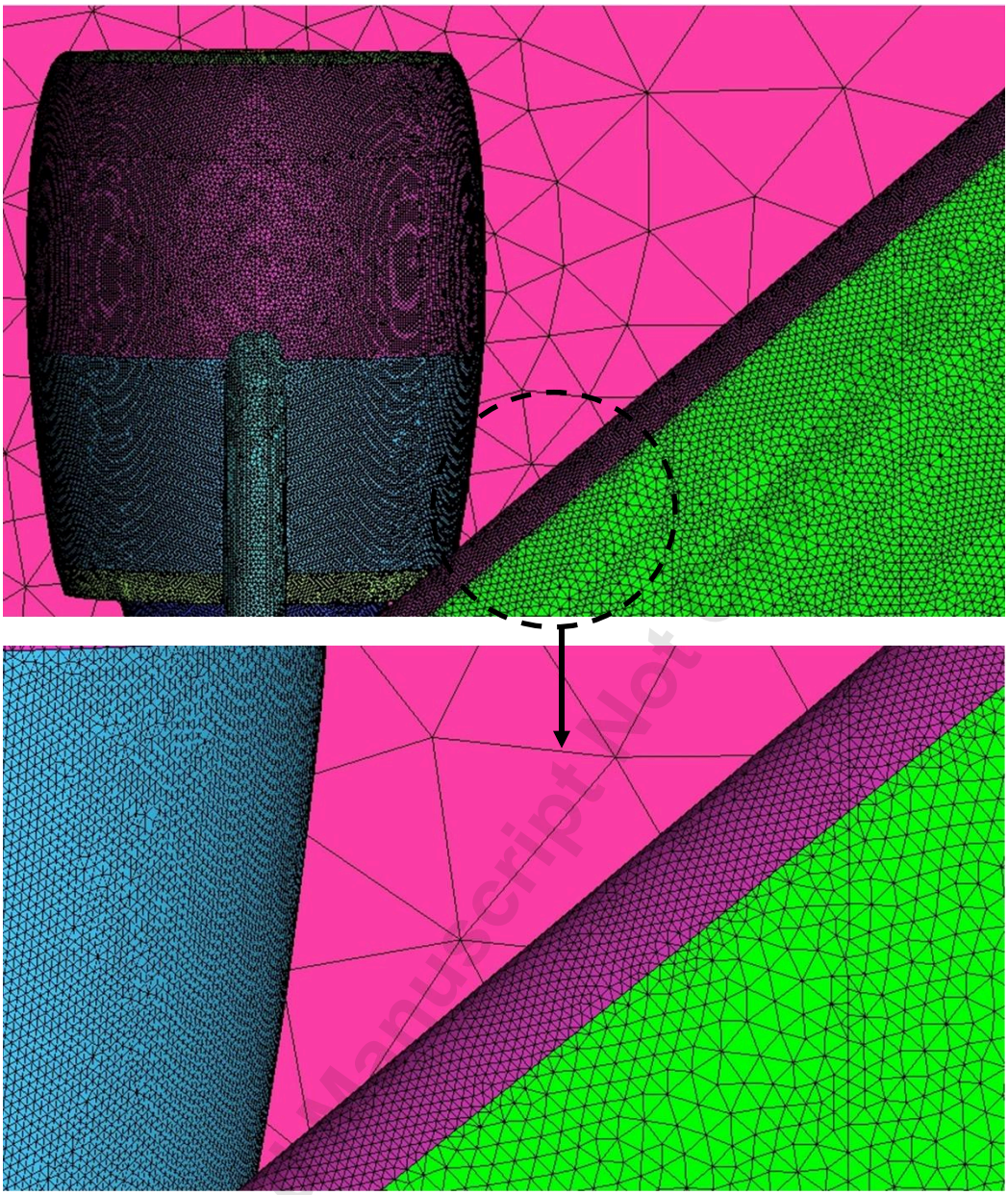

Fig. 7a: Surface mesh distribution around wing/engine assembly. Fig 7b: Shows the magnified view.

The 'prism' elements are important as they signify the boundary layer mesh; 10 boundary layers are used. Figure 8, shows a typical prism mesh for forward thrust configuration. A good prism mesh will restrict the wall Y+ values within the acceptable range. Y+ values are less than 150 for this study.

Volume mesh is important, as it accounts for the external flow physics. A decent far-field mesh is important, to eliminate the numerical reflections. Density blocks are built to refine the volume mesh around the following surfaces: wing leading and trailing edges, fan nacelle inlet, and for the fan and core exhaust nozzles.

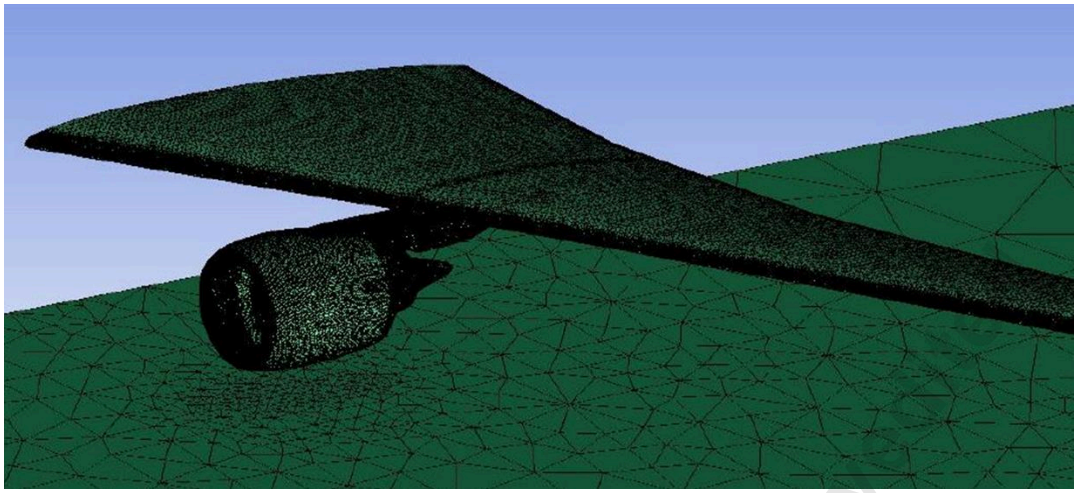

Fig. 8: Typical prism mesh for a reverser in stowed configuration.

2.3 CFD Setup

Commercially available CFD software, FLUENT is employed for all cases investigated within this paper. FLUENT is a finite-volume solver and employs temporal and spatial discretization schemes that provide second-order accuracy in space and time [4]. The CFD investigations presented in this paper are all performed at SLS condition. Pressure based solver is used along with SIMPLE algorithm. 'Air' with ideal gas properties is chosen as the working fluid: the value of 'c_p' and other fluid properties are set accordingly. Realizable k-ε turbulence model is used in all cases; this is in line with previous studies conducted in industry and academia [Ref 5, 6 and 7]. Initially, simulations are started with a low value of fan and core outlet pressures, using first order discretization scheme. After the initial development of the flow, the scheme is switched to the second order upwind scheme. Typically, the steady-state computations are well known and established. The convergence is observed by making sure that the second order residuals remain unchanged; it is ensured that the mass, momentum, and energy residuals are less than 10^{-4}. Mass flow balance criterion is also established for each case by calculating the mass flows for the fan and core inlet and nozzle exit surfaces.

2.4 Engine Performance Data Acquisition

Engine design and off-design performance analyses are performed on a CUTS_TF (Cranfield University Twin Spool Turbofan) engine, which is a HBPR turbofan engine and its characteristics are similar to GE-90. Gas turbine performance simulation software, GasTurb10 [8], is used for the performance analyses. This task is also supported by

the information and data acquired from the public domain [9]. This 1D engine design and off-design exercise provide useful engine performance data which is used to setup boundary conditions for the CFD analyses. Table 1 presents a summary of the typical data set which is established from the engine performance simulations. Of particular interest are the columns of 'Forward Idle Thrust', 'Idle Reverse Thrust' and 'Maximum Reverser Thrust'. These conditions are important, as any large civil aircraft is likely to experience all of them during landing.

From the engine design and off-design performance exercise, values of fan and core inlet and outlet pressures and temperatures are obtained at different power settings. These values are used to setup the boundary conditions for the CFD cases. Further information on the effect of TR deployment on engine performance can be obtained from references [10, 11].

Table 1: Results from the CUTS_TF engine design and off-design performance analyses.

Parameter	SLS Max Power	TO M=0.24	Cruise Alt=10,670m M=0.80	Forward Idle Thrust M=0.211	Idle Rev/Thrust M=0.211	Max Rev/Thrust M=0.211	Units
$\dot{w}$	1467	1521.9	575.7	807.9	944.79	1407.4	Kg/sec
BPR	8.40	8.47	8.1	11.9	11.69	9.5	-
OPR	39.6	39.17	42.96	12.94	15.8	31.6	-
TET	1712	1712	1584	1250	1300	1580	K
FPR	1.39	1.35	1.25	1.03	1.06	1.24	-
Engine outputs from GasTurb							
SFC	8.30	11.04	15.6	11.91	1.94	10.02	g/(kN.s)
$\eta_{Propulsive}$	0.00	0.41	0.76	0.57	0.53	0.40	%
$\eta_{Thermal}$	0.53	0.54	0.59	0.36	0.37	0.52	%
V_{bypass}/V_{Core}	0.82	0.84	0.80	1.23	-	-	-
FNE_{Area}	3.60	3.60	3.60	3.60	3.78	3.78	m^2
CNE_{Area}	1.01	1.01	1.01	1.01	1.01	1.01	m^2
FG_{Thrust}	359.2	385.6	188.8	123.1	-	-	kN
CG_{Thrust}	57.5	60.4	30.4	9.22	12.98	41.6	kN
GR_{Thrust}	-	-	-	-	128.1	263.5	kN
NR_{Thrust}	-	-	-	-	182.6	322.3	kN
GE90-94B technical data available in the public domain (Janes Aero Engine)							
$\dot{w}$	1467	-	576	-	-	-	Kg/sec
BPR	-	8.4	8.1	-	-	-	-
OPR	39.6	-	-	-	-	-	-
s.f.c	8.3	-	15.6	-	-	-	-
$FN_{Gross\ Thrust}$	416.8	-	-	-	-	-	kN

3. Results and Discussion

3.1 Validation of CFD Data

NASA carried out extensive wind tunnel testing for the reverser stowed configurations. The main objective of these tests was to record the static pressure values at different thrust settings and establish an overall performance criterion for a range of Fan Nozzle Pressure Ratios (FNPRs). The availability of the test results is a very useful source and authors have used it to validate the CFD results.

During experiments, static pressure values were recorded on the core external (i.e. PSIFD1-10), fan nacelle internal (i.e. PSOFD1-5), fan nozzle (i.e. PSFEN1-4) and pylon surfaces (i.e. PSPYL1-5) as illustrated in Fig. 9. All experimental values were measured at 14 degrees clockwise from the engine centerline (Fig. 10). To validate the CFD analyses, it is important to maintain consistent comparison with the experiments. Therefore, a cut-plane is created at the same location as that for the experiments i.e. 14 degrees clockwise from the engine centerline.

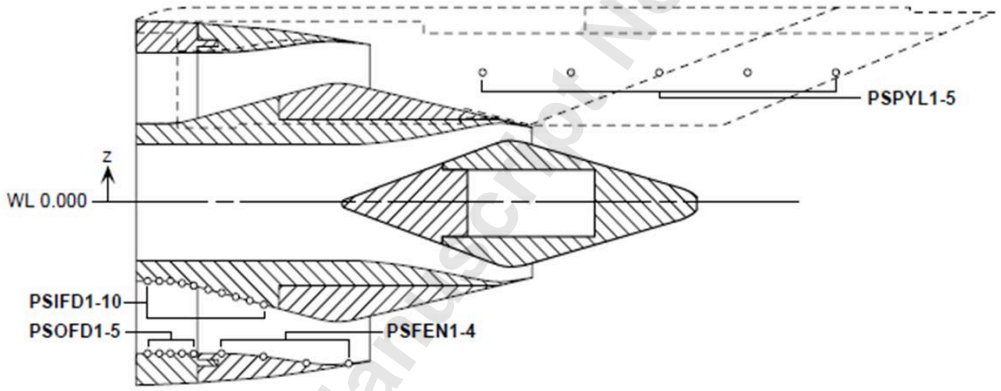

Fig. 9: Static pressure measurement points for a reverser stowed configuration [1].

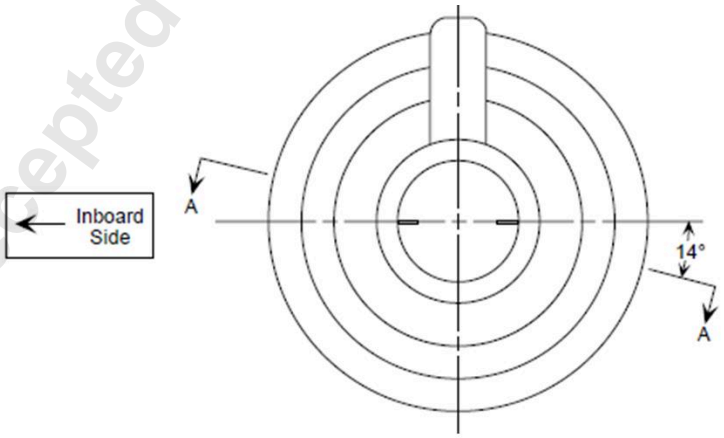

Fig. 10: Static pressure measurements were recorded at 14 degree, clockwise from the engine horizontal centerline [1].

It is evident from Figs. 11, 12 and 13 that the CFD results exhibit good agreement with the experimental data for a range of FNPR values; the difference between the test and CFD results is approximately 2%. The reason for small discrepancies is primarily attributed to the following:

(i) The choice of the turbulence model and measurement errors.

(ii) The CAD models used for the CFD analyses may have some tolerances and may not be the exact representation of the geometry used during experiments.

(iii) In the wind tunnel experiments, the engine was mounted on a stand and many of the tests were performed without a wing; whereas for all the CFD cases, a runway is included and all analyses are performed with the wing installed. Thus, the inclusion of runway and wing may have introduced some discrepancies, specifically on the pylon geometry.

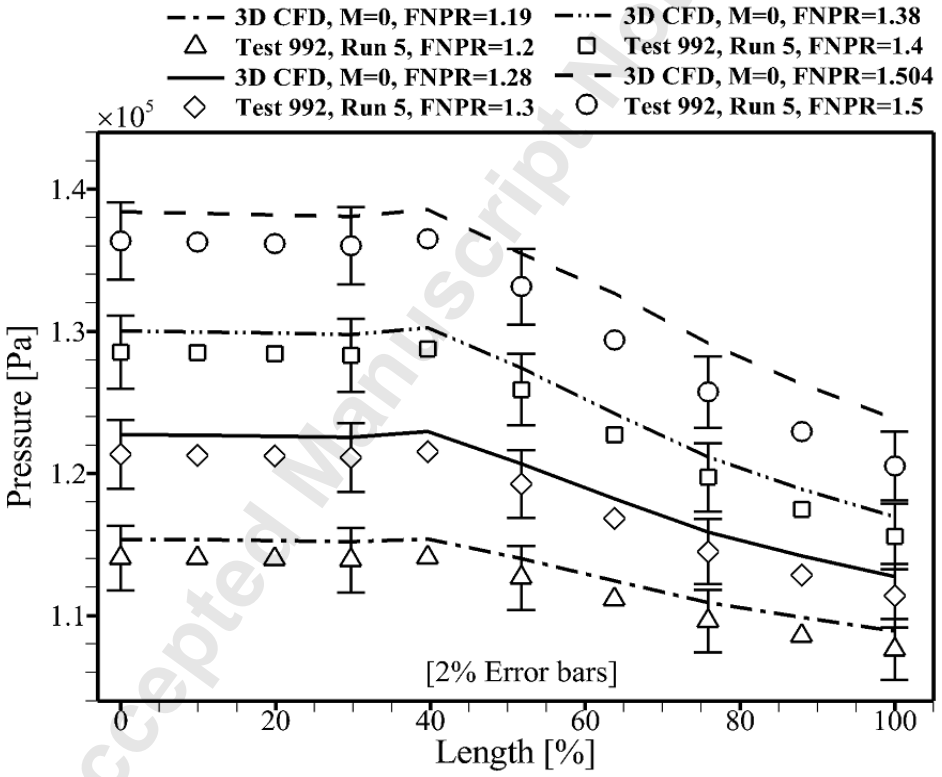

Fig. 11: Comparison of CFD and test data for the core external surface.

Journal of Engineering for Gas Turbines and Power. Received August 17, 2017;
Accepted manuscript posted December 25, 2017. doi:10.1115/1.4038816

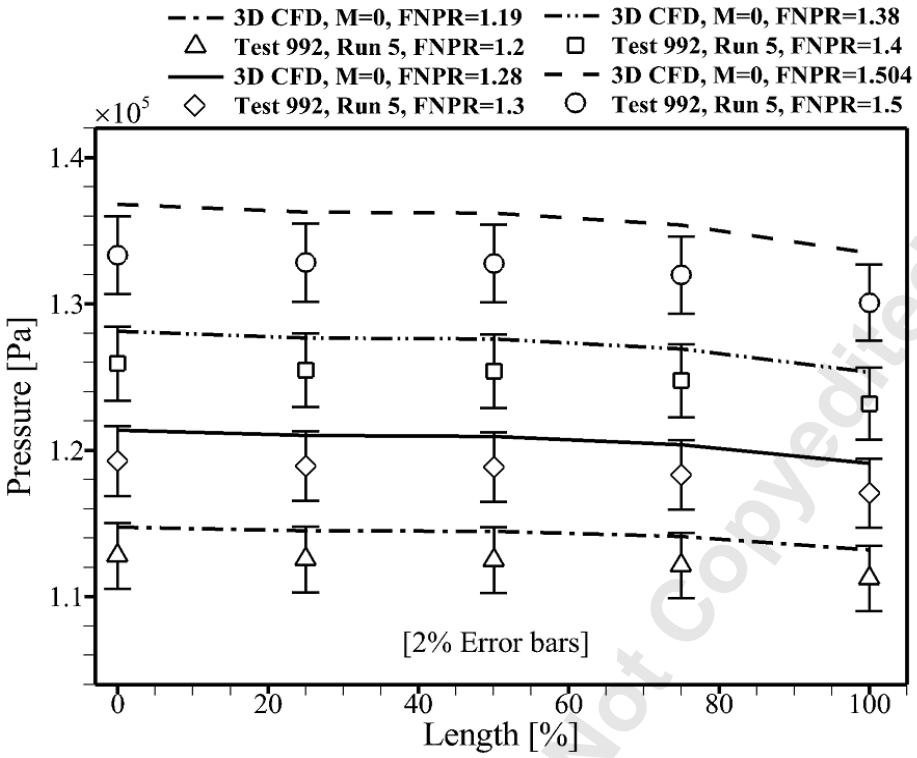

Fig. 12: Comparison of CFD and test results for the fan nacelle internal surface.

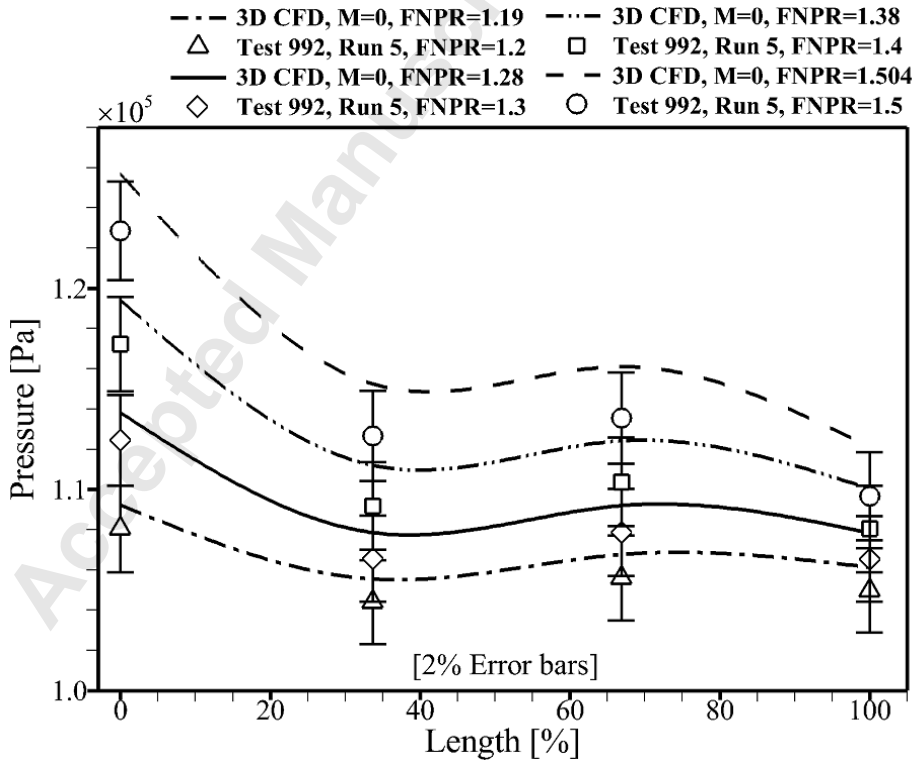

Fig. 13: Comparison of static pressure values on the fan nozzle internal surface.

3.2 Validation of Thrust Estimation

It is essential to have confidence in the engine CAD models. The appropriate method is to obtain the values of the engine fan and core inlets and nozzle exit areas from the design point study. Once the surface area values are set, appropriate boundary conditions are applied to the CFD cases. It is important that the fan, core and overall net thrust values obtained from the 3D CFD analyses are in good agreement with that obtained from the 1D engine performance study.

The engine fan and overall net thrust were measured for all the 3D CFD cases. These values are then compared against those obtained from the 1D performance model: the difference between the two values is less than 10%, (Fig. 14 and 15). The difference is likely due to the following:

(i) Choice of the turbulence model,

(ii) Geometric tolerances in the CAD model.

The values of Fan Gross and Overall Engine Net Thrust are important and will be used in Part 2 to assess the CMTTTR reverser effectiveness.

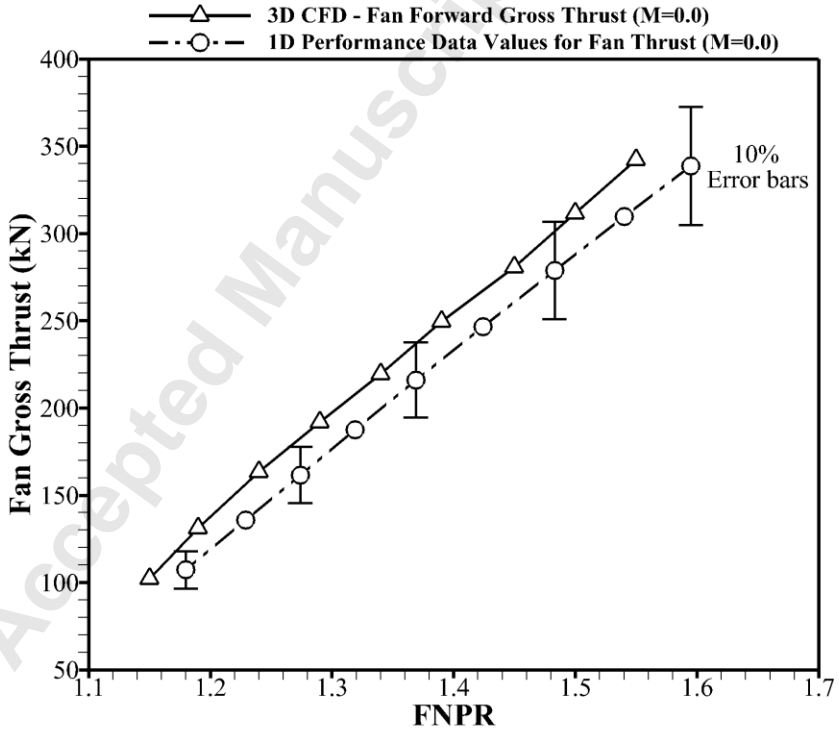

Fig. 14: Comparing CFD and theoretical values for SLS, fan gross thrust.

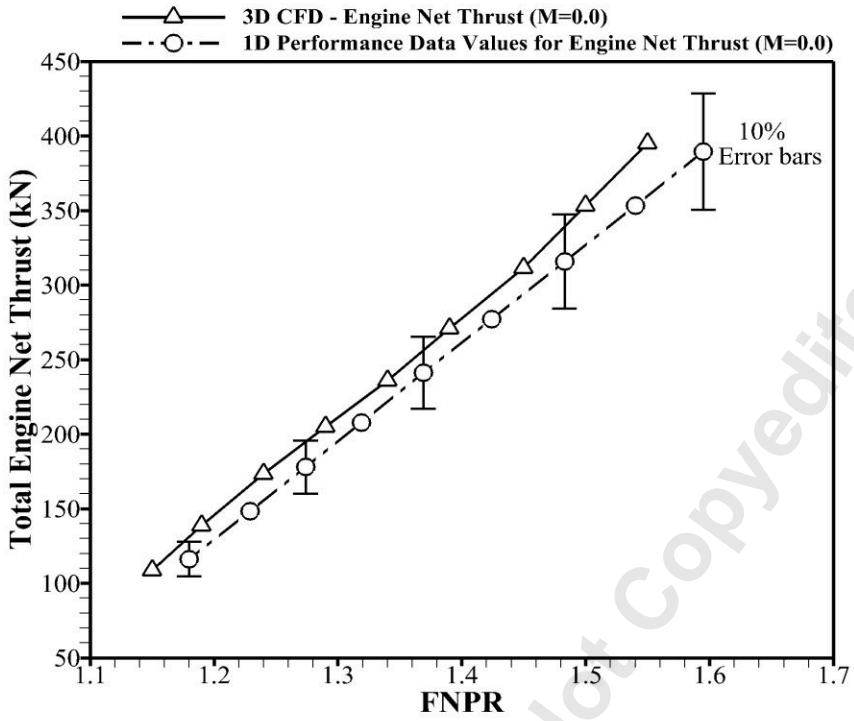

Fig. 15: Comparing CFD and theoretical values for SLS, engine total net thrust.

3.4 Analyses of CMTTTR in Stowed Configuration

This section will facilitate the discussion on the CFD results acquired corresponding to the CMTTTR in stowed configuration (i.e. forward thrust). Several CFD analyses are carried out at different thrust settings each having a different fan and core nozzle pressure ratios. The aerodynamic flow phenomenon discussed here is for the CFD case in which the FNPR≈1.55. Furthermore, NASA performed the wind tunnel experiments for a wide range of FNPRs (i.e. ranging from 1.0 to 2.0), however, from the engine performance study it is observed that for a CUTS_TF engine FNPR>1.6 are not practical at landing conditions and are unlikely to occur in a real scenario. Thus, for this CFD study, FNPRs are limited to 1.6.

Flow visualization, of the 3D model, is presented in Figs. 16 and 17. However, to understand the flow better, streamlines plots are constructed from the CFD results by taking horizontal and vertical cut-planes about the engine centerline. The streamline plots corresponding to a typical FNPR=1.55 are presented in Figs. 18 and 19.

In order to develop a clear understanding of the flow physics and to communicate the results effectively, the flow in the horizontal and vertical streamline plots are divided into 9 zones; 4 zones corresponding to the flow in horizontal

plot highlighted in Fig.18 and the remaining 5 zones correspond to the flow behavior in the vertical plane highlighted Fig. 19. The following section will elaborate on each plane respectively.

3.5 Flow behavior of the CMTTTR as seen on the horizontal plane from the engine center line

The discussion presented here is based on the flow characteristics presented in Fig.18. The area upstream of the engine inlet is referred to as zone 1. The flow is initially widespread, however, as the streamlines approach the engine inlet the flow converges. Thus, the flow is accelerating as it is sucked into engine inlet. There may be an effect due to the CFD far field and also, in reality, due to the aircraft fuselage since at static conditions there is nothing else to stop the air from arriving at the intake from the side of the engine.

The flow in zone 2 and 3 represents the external flow on either side of the engine nacelle. The main reason for there being any flow at all over the nacelle at static conditions is due to the exhaust jets entraining air from the side of the engine nacelle. This is clear from the CFD results. The flow in zone 2 is affected by the symmetric boundary condition. It assumes that there is an engine on either side of the symmetry hence a passage is formed between the two engines. The flow in zone 2 is, therefore, guided flow and is mostly straight.

The flow in zone 3 is unrestricted; the streamlines approach the outer nacelle and the engine exhaust flow at an angle. This is mainly attributed to the suction momentum created at the engine inlet and also due to the high exhaust velocities of the engine jets (i.e. from fan and core), which causes air to be entrained from the free stream. Therefore, it is reasonable to consider that the flow in zone 3 is dependent mainly on the engine thrust settings; any variation in engine power will affect the flow behavior in the engine inlet and exhaust regions which in turn will affect the streamlines in zone 3.

The flow in zone 4 represents the engine exhaust flows (i.e. fan and core). The streamlines are straight primarily due to the high exit momentum.

3.6 Flow behavior of the CMTTTR as seen on the vertical plane from the engine center line

The discussion presented here is based on the flow characteristics presented in Fig. 19. The flow in zone 5 is broadly similar to that observed in zone 1, the only difference being that the line of symmetry has changed, due mainly to the close proximity of the ground. In the flow, some 8 m ahead of the engine, the streamlines are widespread. The flow momentum is low; however, as this flow approaches the nacelle inlet the air accelerates (i.e. the streamlines are compressed). Some flow separation is observed at the inside of the fan nacelle lip cowl, mainly because the flow is

turning more aggressively (see Fig. 19). The vertical plane shows that the top side has a far-field boundary condition and the bottom side has a runway, resulting in the streamlines adopting a 'D' shape.

The flow in zone 6 is influenced by zone 5, the jet entrainment and the blocking effect of the wing. This results in the streamlines of Zone 6 approaching the nacelle and pylon upper surfaces at an angle (behavior of the streamlines is thrust dependent). This flow then accelerates some small distance before some of it reaches a halt at the wing leading edge. The stagnation point is on the wing upper surface, between the boundaries of zone 6 and 7. This flow then splits either side of the pylon.

The flow in zone 7 is influenced by the entrainment effect of the exhaust jets. The streamlines in Zone 7 show that some part of the flow will approach the wing suction surface: however, as this flow approaches the wing, part of it will turn and accelerate aggressively towards the wing trailing edge. This high momentum flow from the wing trailing edge will react with the outer periphery of the engine exhaust jet. Thus, a flow boundary will form, where the inner region will be the engine exhaust flow. The top section of the engine exhaust flow will mostly be shielded by the high momentum flow departing the wing trailing edge. The remaining low momentum free stream flow in zone 7 will approach at high angle and is similar to what was observed for zone 3.

The streamlines in zone 8 represent the flow behavior between the engine nacelle and the runway. The flow behavior is similar to what was observed for zone 2, the only difference being, instead of the symmetry, this time a passage is formed between the nacelle bottom surface and the runway, which causes the flow to be uniform and straight. The upper region of the flow in zone 8 will be entrained by the bottom half of the periphery of the engine exhaust flow. The engine exhaust flow in zone 9 is almost straight and uniform. The characteristics of the flow formed in zone 9 are similar to what was observed for zone 4.

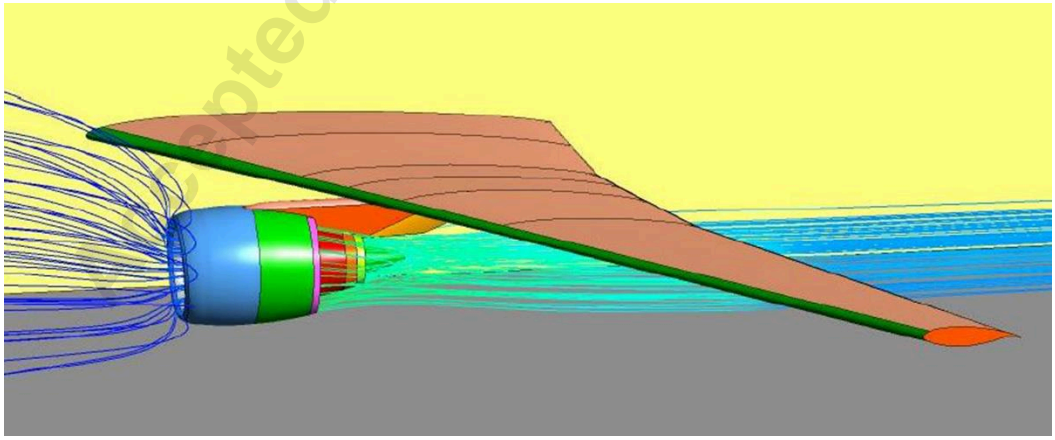

Fig. 16: CFD analyses showing the engine inlet and exhaust flows, FNPR=1.55, M=0.0.

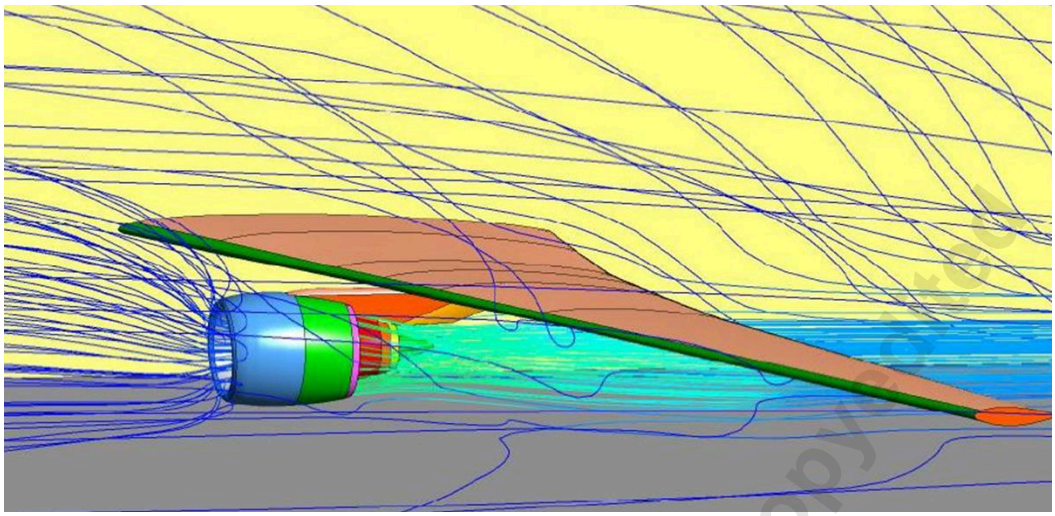

Fig. 17: CFD analyses showing the engine inlet, exhaust and free stream flows, FNPR=1.55, M=0.0.

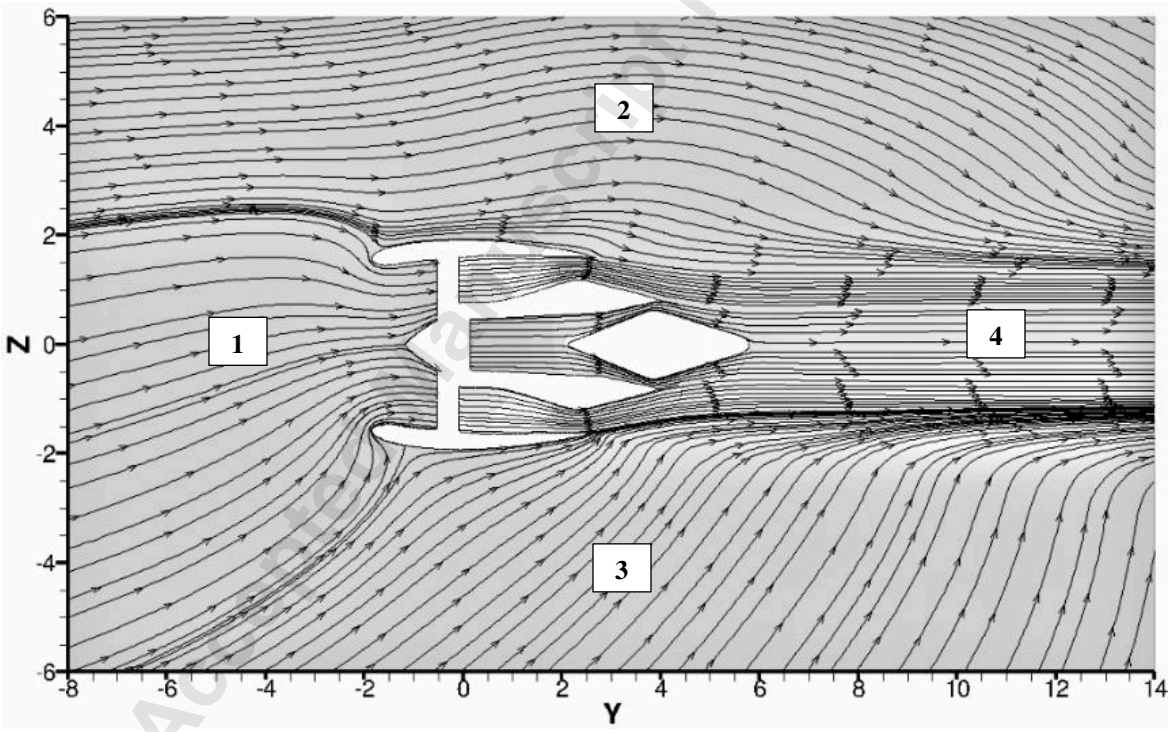

Fig. 18: Streamlines plot in the horizontal plane, FNPR=1.55, Mach=0.0.

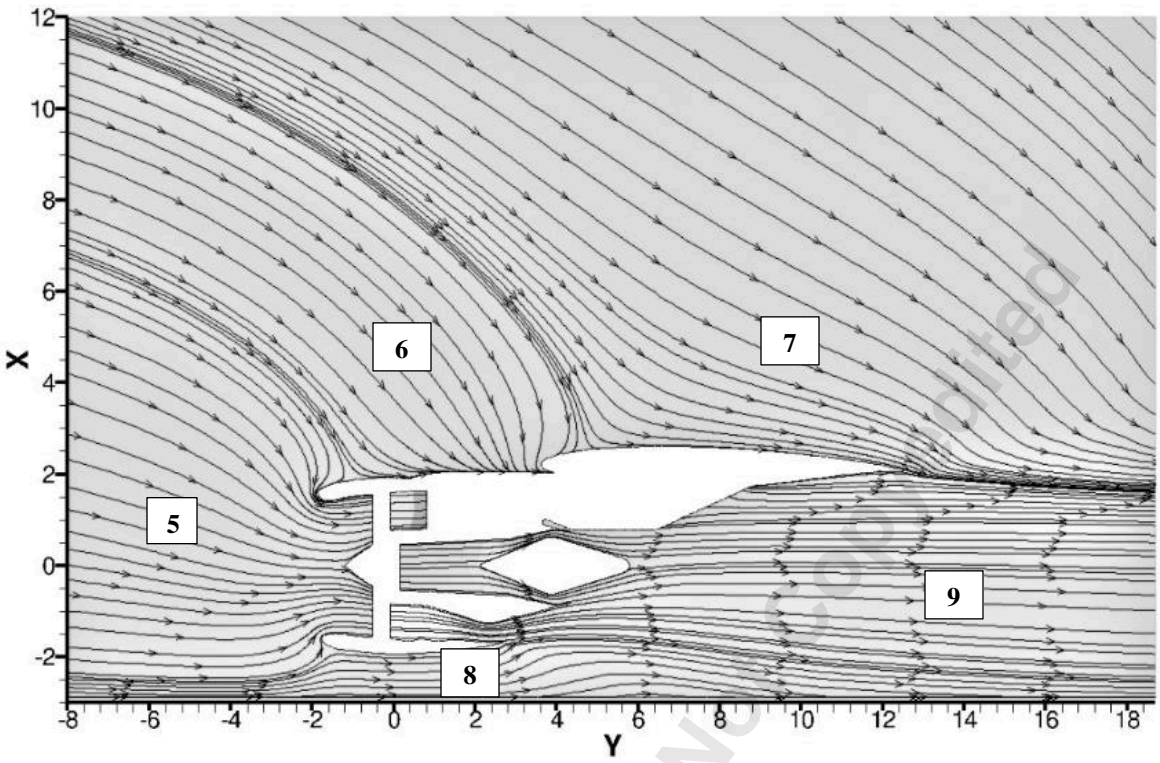

Fig. 19: Streamlines plot in the vertical plane, FNPR=1.55, Mach=0.0.

4. Conclusion

An extensive assessment of a Core Mounted Target Type Thrust Reverser (CMTTTR) design in stowed configuration is presented in this paper. The results are based on the successful implementation of the 3D CFD analyses of an integrated (engine, pylon, and wing) design, modeled after a representative modern civil aircraft configuration, operating at SLS condition. A comprehensive validation of the acquired CFD results was carried out against the experimentally derived results reported by NASA. The acquired results exhibit good agreement with the experimental data. Furthermore, the performance characteristics of the employed engine CAD model was validated by comparing the thrust values obtained from the 3D CFD study against the data acquired through 1-D simulation of the employed engine model. The acquired performance values will be adopted in Part 2 of this paper, where the reverser efficiency and performance will be assessed in deployed configuration. Finally, flow characteristics corresponding to the reverser stowed configuration at static conditions are thoroughly examined and discussed based on the 2D horizontal and vertical streamline plots.

5. Acknowledgments

This work was supported by Cranfield University, Centre for Propulsion Engineering. The main author would like to thank and acknowledge Anthony Jackson for his guidance and significant expertise in engine design, performance and aerodynamics. Special thanks to Vishal Sethi for his guidance and supervision of this complex project. Thanks to Bidur Khanal for his knowledge and expertise in CFD and post processing. In the end, special thanks to Fakhre Ali, for his valuable suggestions and advice on turbomachinery design and performance.

References

[1] Scott C. A., "Static Performance of Six Innovative Thrust Reverser Concepts for Subsonic Transport Applications: Summary of the NASA Langley Innovative Thrust Reverser Test Program", TM-2000-210300, NASA - Langley Research Centre, Hampton, Virginia

[2] Yetter, J. A., "Why Do Airlines Want and Use Thrust Reversers? – (A compilation of Airline Industry Responses to a Survey Regarding the Use of Thrust Reversers on Commercial Transport Airplanes)", TM – 109158, NASA - Langley Research Centre, Hampton, Virginia.

[3] "Results from two surveys of the use of Reverse Thrust of Aircraft Landing at Heathrow Airport" – British Airways / BAA Heathrow, Environmental Affairs / Airside Environment.

[4] FLUENT 6.3 User's Guide. Fluent Inc, 2006.

[5] Chuck. C., "Computational Procedure for Complex Three-Dimensional Geometries Including thrust Reverser Effluxes and APUs"., AIAA-2001-3747., 37th AIAA Joint Propulsion Conference, 8th – 11th July, 2001, Salt Lake City, Utah.

[6] Andrade. F. O., Ferreira. S. B., Silva. L. F. F. Jesus. AA. B., Oilveira. G. L., "Study of the Influence of Aircraft Geometry on the Computed Flowfield During Thrust Reverser Operation"., 24th AIAA Applied Aerodynamic Conference, 5th – 8th June, 2006, San Francisco, California.

[7] Trapp. L. G., and Oliveira. G. L., "Aircraft Thrust Reverser Cascade Configuration Evaluation Through CFD"., 41st AIAA Aerospace Meeting and Exhibition, 6th – 9th January, 2003, Reno, Nevada.

[8] Gas Turbine Performance Software, "GasTurb 10", GasTurb GmbH.

[9] Jane's Publication, "Jane's Aero Engines".

[10] Mahmood. T., Jackson. A., Sethi. V., Pilidis. P., "Thrust Reverser for a Separate Exhaust High Bypass Ratio Turbofan Engine and its Effect on Aircraft and Engine Performance", GT2011-46397, ASME 2011 Turbo Expo – Vancouver, Canada.

[11] Mahmood, T., Jackson, A., Rizvi, S. H., Pilidis, P., Savill, M. and Sethi, V., "Thrust Reverser for a Mixed Exhaust High Bypass Ratio Turbofan Engine and its Effect on Aircraft and Engine Performance", GT2012-68934, ASME 2012 Turbo Expo – Copenhagen, Denmark.

[12] Google.com (2017); searched, thrust reverser presentation, URL: http://slideplayer.com/slide/1462344/., last visited (26-June-2017).

2017-12-25

CFD investigation of a core-mounted-target-type thrust reverser, Part 1: reverser stowed configuration

Mahmood, Tashfeen

ASME

Mahmood T, Jackson AJB, Sethi Vi et al., (2018) CFD investigation of a core-mounted-target-type thrust reverser, Part 1: reverser stowed configuration. Journal of Engineering for Gas Turbines and Power, Volume 140, Issue 9, September 2018, Article number 091204

http://dx.doi.org/10.1115/1.4038816